



Work  
Smarter.

## TABLE OF CONTENTS

<b>INTRODUCTION/BACKGROUND</b>	<b>2</b>
<b>"GOLD STANDARD" COUNT ACCURACY</b>	<b>3</b>
<b>SUPERIOR CELL VIABILITY MEASUREMENTS</b>	<b>4</b>
<b>COULTER PRINCIPLE DETECTION - UNPARALLELED SIZE RESOLUTION</b>	<b>6</b>
<b>METRICS FOR EVALUATING SAMPLE PURITY</b>	<b>7</b>
<b>PRECISE/ACCURATE NUCLEI COUNTS</b>	<b>9</b>
<b>ROBUST CELL PHENOTYPING</b>	<b>9</b>
<b>SUMMARY</b>	<b>10</b>

## Introduction/Background

10x Genomics (10x) has revolutionized genomic analysis by introducing capabilities for studying gene expression at the single-cell level. Previously, genomics studies had been limited to bulk analysis of tissue samples. Such analysis was naturally limited due to the polydispersity of the cells in the tissue. As an illustrative example, 10x often identifies the well-known, wide array of cell types that inherently comprise blood samples<sup>1</sup>. Analysis of those samples in bulk is complicated not only by the diversity of the various cell types and phenotypes, but also from the shifting proportions of cell types (particularly in pathological states). As another illustrative and frequently-studied example, cancerous tissue will contain not only the healthy functional cells, stem cells, and stromal cells, but it will likely also contain the mutated cancerous cells and infiltrating lymphocytes<sup>1</sup>. The 10x hardware (Chromium Controller and accessories) and software solutions address these challenges by providing researchers with capabilities to reliably generate barcoded, isolated single-cell genomic libraries for downstream sequencing. Along with the 10x software analysis, this allows for the full discrimination of the individual population genomics and sub-population expression profiles.

As part of their quality control (QC) guidance, 10x emphasizes the critical needs in sample preparation, including the absolute necessity for precise measurements of cell concentrations, viabilities, and for determination of the aggregation/clustering composition of the samples<sup>2</sup>. These parameters are highly deterministic in the success vs. failure of the genomic analysis. Improper preparation can result in significant lost time and cost (~\$2000-\$3000/sample in 10x processing alone<sup>3,4,5</sup>) as well as ambiguity and error in data interpretation. These repercussions are significant, not only for the quantifiable time and money involved, but also for the intangible, "opportunity" costs associated with the expenditure of often scarce tissue samples.

Orflo Technologies' (Orflo) Moxi GO II cell health system (**Figure 1**) is ideally and uniquely suited to stringently fulfilling these 10x sample preparation requirements. The system combines the Coulter Principle, the recognized gold standard for precise cell sizing and counts, with simultaneous fluorescent measurements using a 488nm laser, coupled with two photomultiplier tube (PMT) detection channels. The first fluorescent channel is filtered to detect fluorescence emissions at 525/45nm and the second is user-swappable to detect emissions at either 561nm/LP or 646nm/LP (depending on experiment needs). This fluorescence configuration is ideal for many of the most common fluorophores including FITC (immunolabeling, Annexin V), Phycoerythrin (PE, immunolabeling, Annexin V), Propidium Iodide (PI for viability), Calcein-AM (Cell Health), and GFP (transfection efficiency).

The Moxi GO II utilizes a disposable flow-cell architecture, does not require system warm-up, runs tests in under 10 seconds, and does not require cleaning/shutdown procedures. Its low cost and very small footprint make it easy for researchers to acquire one for their own lab, placing it on the bench-top or even in the cell culture hood. These characteristics enable researchers to easily and frequently QC and characterize



**Figure 1 – a.)** Orflo's Moxi GO II – Cell Health Analyzer. Image shows user loading a sample into the two-test disposable flow cell. The Moxi GO II is a flow cytometer/cell health analyzer with a 488nm laser and two fluorescence recording channels (2 PMT's with emission filters at 525/45nm filter and a user-swappable 561nm/LP or 646nm/LP). **b.)** Two-test, disposable flow cell "cassette"

their 10x samples. More importantly, beyond convenience and ease-of-use, the system delivers “gold standard” count accuracy, superior viability measurements, unparalleled size resolution, metrics for evaluating sample purity, accurate nuclei counts, and robust cell phenotyping capabilities. The quality and depth of the QC output of the Moxi GO II, along with its simplicity of operation cannot be matched by any other system in its price range. The result is an affordable 10x QC system that delivers comprehensive 10x QC analysis on-demand, with the highest quality data output. The data outlined the application note below is designed to describe the clear advantages of the Moxi GO II for 10x QC applications, organized by each individual QC metric.

### “Gold Standard” Count Accuracy

The Moxi GO II system implements an impedance-based (electrical) measurement technique (Coulter Principle), not an imaging one, for counts and sizing. The Coulter Principle has long been regarded as the “gold standard” for particle counting due to its accuracy and precision. **Figure 2a** demonstrates that the Moxi system matches (linear fit,  $r^2 > 0.98$ ) the performance of the highly regarded Beckman Coulter Z2 system by comparing counts of serial dilutions of a range of particle types (beads, yeast, mammalian cells) and sizes (~4µm to ~16µm in mean diameter). This impedance-based technique involves generating a

true, **volumetric** measurement of **each individual cell/particle** as it passes through a precision-drilled aperture. This volumetric measurement of particles is huge differentiator versus the image-based analysis that underlies the vast majority of competitive cell counting technologies. Those systems take an image of the cells and use a software algorithm to interpret the images, effectively “looking for circles”. The inherent flaws of that approach results in counts that will be consistently off and highly variable. Specifically, smaller debris are frequently counted as cells and larger debris are often treated as clusters of cells. Furthermore, in contrast to the Moxi GO II that can count up to 40,000 cells in the span of a few seconds, imaging approaches count only up to a couple of hundred cells per test. The increased cell count for the Moxi GO II greatly contributes to the statistical reliability and precision of the data. In fact, in direct comparison studies, we have found the count error levels (using a Beckman Coulter Z2 system as the reference standard) to be on the order of 10-35% for imaging systems vs. just 5% for the Orflo system (**Figure 2b**). Furthermore, the count-to-count variability, as measured by the coefficient of variation (CV), was on the order of 20-30% for the imaging system compared to 4% for the Moxi system (**Figure 2b**). These advantages are precisely the reason that the Coulter Principle is regarded as the “gold standard” for counting and sizing of particles of all types,

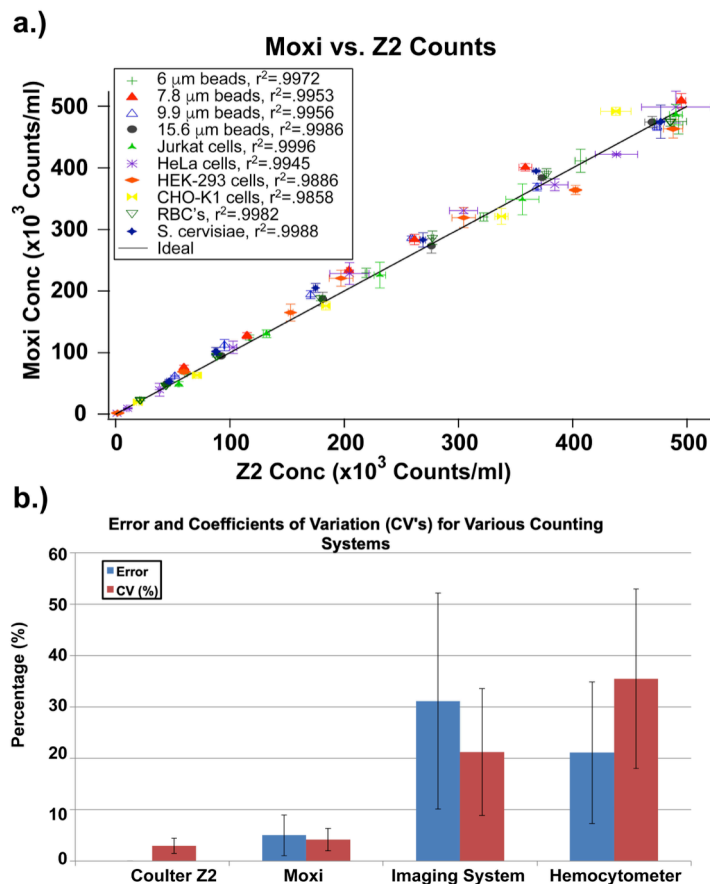


**Figure 2 – a.)** Serial dilution data comparing measured concentrations on the Moxi system to the Coulter Z2 system. Numerous particle types were tested ranging from beads to yeast to mammalian cells. Linear fits of the data show the high correlation between the systems ( $r^2 > 0.98$ ). **b.)** Bar charts of count error (as percentage vs. the Coulter Z2 system) and count CV percentages, by system. The Moxi values are analogous to those of the gold standard Z2 system. The imaging approaches reflect the very high error and variability that are commonly associated with visual analysis.

including cells. And, it is this accuracy that uniquely enables the Moxi GO II to ensure exact cell concentrations for downstream 10x processing.

### Superior Cell Viability Measurements

The Moxi GO II system is unique in combining simultaneous fluorescent measurements with the Coulter-Principle size and count measurements. The system laser and optical configuration enables the industry-standard Propidium Iodide (PI) - based measurements of viability through evaluation of cell membrane integrity. PI is a cell-impermeant nucleic acid stain that is a reference standard for viability measurements due to the large (>50x) shifts in fluorescence intensity that it exhibits when binding with the DNA of dead cells. The difference in PI-based viability discrimination vs. Trypan Blue (Trypan) - based discrimination (the default for imaging approaches) is readily observed in **Figure 3**. An identical Jurkat E6-1 culture was prepared with both PI staining and Trypan staining. **Figure 3a and b** show a view of an identical PI-stained cell region with **(a)** and without **(b)** the PI filter. Referring to the brightfield image **(a)**, it is evident that with the PI filtered output **(b)**, the live cells (that exclude the PI) cells are not at all visible with the naked eye. This highlights the huge difference in signal that is generated between live and dead cells using the PI staining approach. That same sample run on the Moxi GO II yields a dramatic signal difference (**Figure 3c**, 131x separation) between the live and dead cells. In contrast, Trypan staining of the same sample (**Figure 3d**), has a great deal of ambiguity in both the recognition of cells (vs. debris) as well as in the final determination of the live vs. dead cells (due to the varying degrees of Trypan shading). While this ambiguity would be challenging for a trained researcher to discriminate, it is even more difficult to capture with the rigid approach of image-processing algorithms that are employed by many other systems. Ultimately, that contributes to the error and variability in methods that use the traditional imaging approaches. As an example, **Figure 3e** shows the output from a well-known, commercial imaging system that was loaded, per the manufacturer specifications, with a trypan-stained 3T3 cell sample. As the system annotation (red and green circles) shows, even with the small sample size (limited by the field of view of the system), several errors (both false positive and false negative) were made (see arrows).

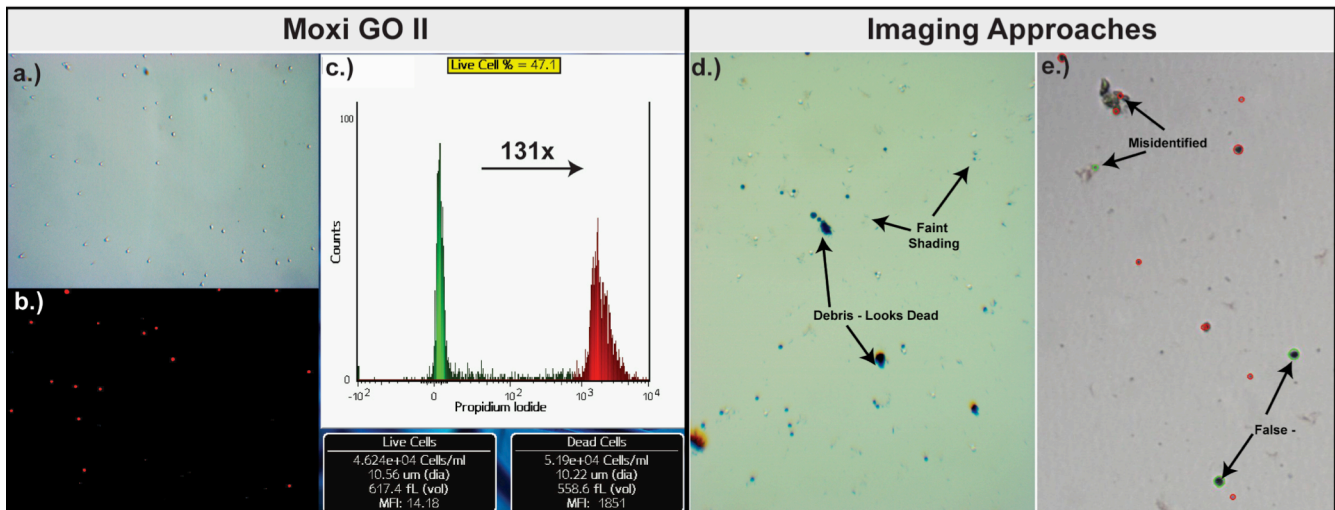


**Figure 3 – a.)** Brightfield microscope view of PI-labeled Jurkat E6-1 cells. **b.)** Equivalent view of the cells with the PI-filter enabled. Note the live cells are no longer visible. **c.)** The PI fluorescence histogram output on the Moxi GO II for the same Jurkat sample. The huge (131x) fluorescence shift simplifies the discrimination of live vs. dead cells. (47.1% viability). **d.)** The same Jurkat sample stained with Trypan Blue and viewed with brightfield microscopy. The presence of debris and the faint shading differences of Trypan make both cell identification and live/dead discrimination challenging. **e.)** A separate Trypan labeled 3T3 sample processed on a leading imaging system. The annotation of live and dead cells by the system show several errors, even in the very small cell subset analyzed by the limited field of view of the system.

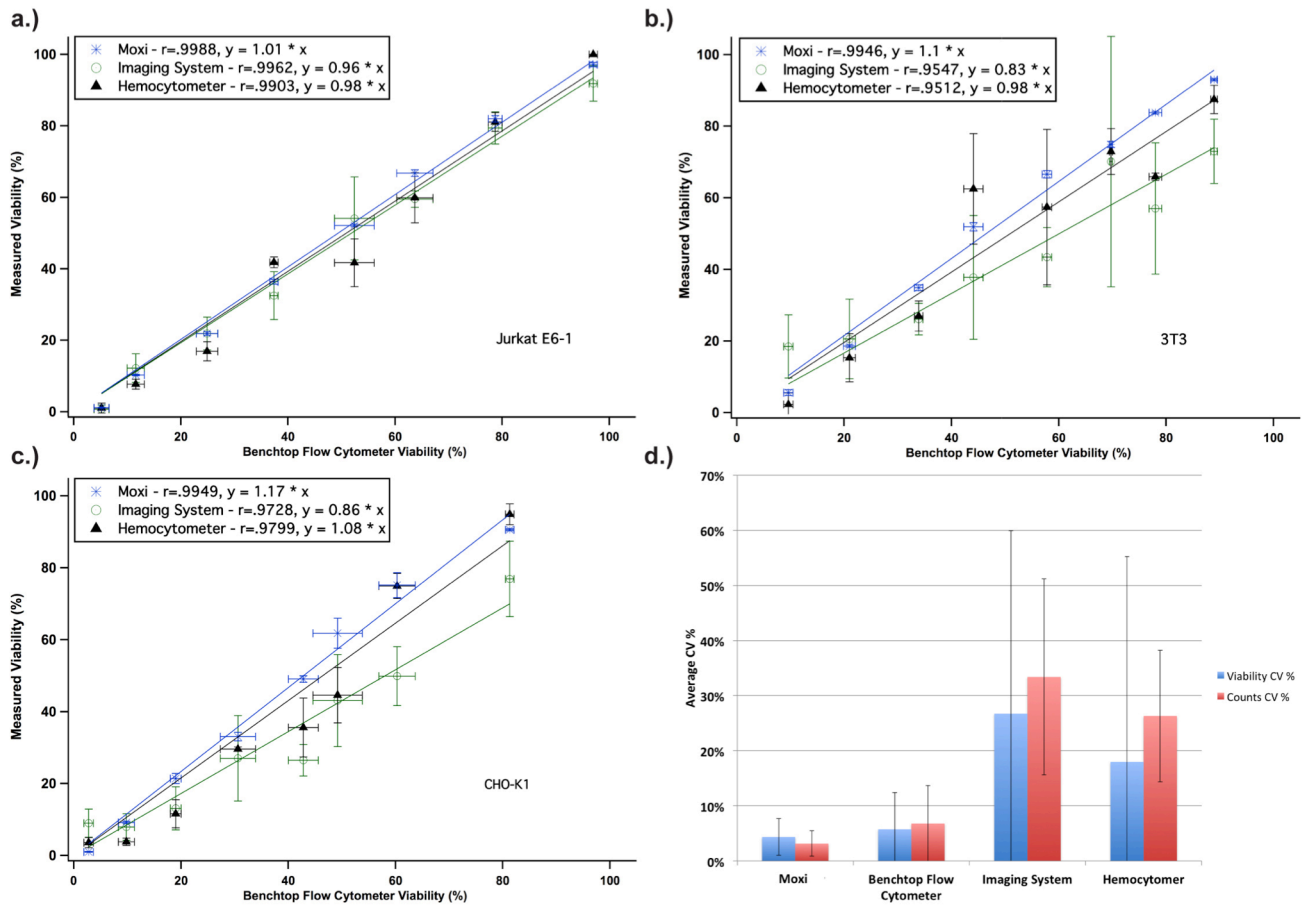


**Figure 4** – Comparisons of Moxi system, imaging system and hemocytometer measured viabilities to a benchtop flow cytometer viability measurement for three cell lines (**a.**) Jurkat E6-1, **b.**) 3T-3, and **c.**) CHO-K1 cells). Controlled viability levels were created through ratiometric mixing of healthy and heat-killed (60C, 15min) cell samples. The Moxi system significantly outperformed the Trypan-Blue based systems based on linear fit and variation (standard deviation) of measurements. **d.)** Average coefficients of variations (CV's) percentages for both counts and viability measurements across all systems. Error bars represent +/- one standard deviation.

Aside from the obvious qualitative differences, the improved quality of the Moxi viability data can also be quantitatively evaluated, as shown in **Figure 4**. Viability levels for three different cells types (**a.**) Jurkat E6-1, **b.**) 3T-3, and **c.**) CHO-K1 cells) were concurrently measured with the Moxi System, a commercial benchtop flow cytometer, a commercial imaging cell counter, and the hemocytometer approach. Seven theoretical viability levels were created through ratiometric (live/dead ratios of 1.0, 0.85, 0.7, 0.55, 0.4, 0.25, 0.1, 0.0) mixing of healthy cells with dead (heat-killed, 60°C, 15min) cells. For the image-based approaches, cells were stained with Trypan (50/50 mix of cells with 0.4% Trypan solution, 1min incubation). For the Moxi and benchtop flow system, cells were labeled with PI (2µg/ml, 5min incubation). Data points for each sample were collected in triplicate with each of the instruments and in duplicate (2 wells, 8 large (1 mm<sup>2</sup> squares)) for the hemocytometer. In comparing the linearity (**Figure 4, a, b, and c**, linear fit with Pearson's r values) and CV's (**Figure 4d**) for the Moxi system counts and viability to that of the other systems, the Moxi system outperforms all systems, including the high-end flow cytometer. In using the benchtop flow cytometer as a reference standard, the Moxi system significantly outperformed the Trypan approaches in both linearity and variability. Given the critical need for accurate viability measurements in QC of 10x preparations, the accuracy and consistency of the Moxi GO II viability measurements provide another compelling argument for the necessity of the system in 10x cell sample QC.

**Coulter Principle Detection - Unparalleled Size Resolution**

In implementing the Coulter Principle as the underlying counting technology, the Moxi GO II measures the exact volume of the particles passing through the detection zone. This approach stands in stark contrast to 2D image analysis for size estimation (used by other cell counters) in which the “circle finding” algorithms are used to try find cells, estimate cell boundaries, and determine a diameter. In addition to the inherent uncertainty of visually determining precise cell boundaries from potentially asymmetric particles with transparent cell membranes, those approaches also are susceptible to the (mis-)identification of 2D debris profiles as cells. In contrast, with a volumetric electrical measurement, the Moxi GO II can better distinguish between 2D particle profiles and cells, determine an exact particle size, as well as generate a much finer resolution of all the measured particles. The overall result is a detailed profile of the cell sample size distribution. The contrast between the approaches is clearly illustrated in **Figure 5** by comparing an equivalent 5-bead size (4.1µm, 6µm, 7.9µm, 10.1µm, and 16µm diameters) sample run on the Moxi system and on a leading image-based cell counting system. The Moxi output (**Figure 5a** - Top Histogram)) clearly resolves all five bead peaks/sizes. The imaging system shows only two of the five peaks (**Figure 5a** - bottom

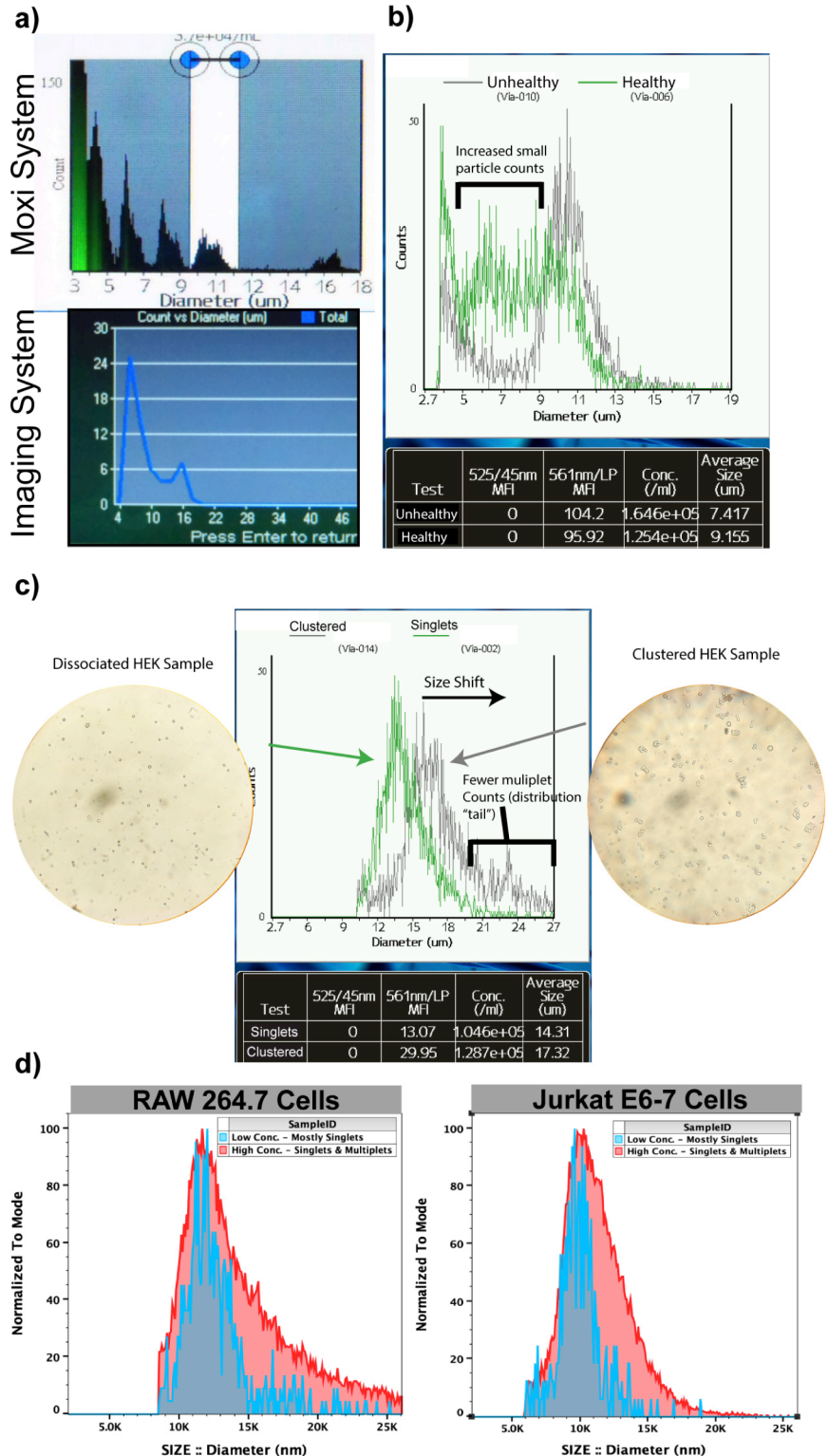


**Figure 5** – a.) Sample with five different sized beads run on Moxi system (top) vs. imaging system (bottom), highlighting the comparative size-resolution of the systems. b.) Moxi GO II on-system size histogram overlay comparing a healthy (gray) Jurkat sample to an unhealthy (green) one. c.) Comparison of poorly dissociated (clustered, gray curve, right image) cell sample to a fully dissociated (singlets, green curve, left image) sample. Note the increased tail length and size shift/increase with the clustered result d.) Mode-normalized curves comparing high concentration (~1.75e6 cells/ml, red curve) cell size histograms to low concentration (~1e5 cells/ml, blue curve) ones. The passage of multiple cells, analogous to clustering, is shown in the increased skew (longer tail) of the distributions.

histogram) with the first four (smaller) bead sizes merging into a single peak.

Practically, this increased size resolution translates to greater insights in the cell sample that can be critical for downstream 10x processing. To illustrate one such example, Figure 5b shows a direct comparison of the size-profile of a “Healthy” Jurkat cell sample vs. an “Unhealthy” (maintained in a hypoxic, room temperature environment for a couple of days) Jurkat sample. With the unhealthy sample, a dramatic shift in the size distribution is evident with a notable increase in the smaller particle counts (~4-9 $\mu$ m in this case) and decrease in the overall mean cell diameter (**Figure 5b** table). The cell size decrease and increase in particle counts are expectedly associated with the disintegration of cells during necrosis. Significantly for 10x applications, this detail in the size profile can be an important indication that there is free DNA/RNA in the media from the lysed cells. Such a composition could very easily compromise sequencing results as those isolated fragments would get trapped into the 10x bead emulsions along with the cells. While this analysis is somewhat qualitative, it still provides valuable insights to the researcher that is uniquely enabled by the precise sizing of the Moxi GO II.

This size resolution also provides the researcher a means of critically evaluating the degree of clustering or aggregation of their cell samples. The 10x protocols emphasize the importance of achieving single cell suspensions prior to processing. The intuitive need for preventing aggregation derives from the need to ensure that only one cell is trapped in each oil droplet. To illustrate the utility of the size distribution in tracking the degree of aggregation, **Figure 5c** (center image) shows the direct comparisons of the Moxi GO II size histogram outputs (using the built-in test comparison/overlay functionality on the system) an aggregated HEK-293 cell sample compared to that of a mostly dissociated (single cell) sample. Specifically, the aggregated tests represented cells that were processed following cell detachment with Accumax, using a basic 10-minute detachment/incubation period and a fixed 10x trituration with a 10ml pipettor. The dissociated cells were generated from the same HEK-293 sample by applying longer protease (1+ hour, Accumax) incubation followed by more rigorous mechanical disruption (gentle vortexing and pipette trituration). In **Figure 5c** (center image), the gray curve (aggregates) shows not only a significant increase in the skew (longer tail) of the distribution but also has a modal peak increase as the sample is predominantly composed of multiplets (clusters of cells) with few singlets (single cells). Callouts from the curves to micrographs show the images of the very samples run during the tests, useful as a secondary verification of the degree of clustering in the samples. In an alternative representation of the same concept, the mode-normalized size histograms for high-concentration (~1.75e6 cells/ml, red curves) samples vs. lower concentration (~1e5 cells/ml, blue curves) are shown in **Figure 5d** for 3T3 cells (left) and Jurkat cells (right). At higher concentrations, multiple cells will periodically pass through the detection zone simultaneously, registering as an effectively larger cell. Qualitatively, as shown in these figures, this is measured from the population skew, showing as an elongated tail extending from the singlet (single cell) cluster. While 10x samples would not ordinarily be run at the higher concentrations, this provides a controlled method for demonstrating the utility of monitoring both the mean cell diameter and the shape of the size distribution. Using those size profiles, researchers can make informed decisions as to the degree of single-cell-dissociation and make the appropriate adjustments to the sample prior to committing to costly downstream 10x processing and sequencing runs.

### **Metrics for Evaluating Sample Purity**

A key component of the 10x cell preparation process is the isolation of single cells into oil emulsion droplets. It follows that, when a researcher is interested in a particular cell type, maximizing the fraction of droplets containing cells of that type is statistically important. The Moxi GO II allows for the evaluation of the sample purity through both size and fluorescent measurements. At the simplest level, the precise size-resolution of the Coulter Principle-based sizing of the system, allows for rapid discrimination of cell types and purity in some samples. **Figure 6a** shows a scatter plot of PE fluorescence vs. cell diameter for a Ficoll-purified

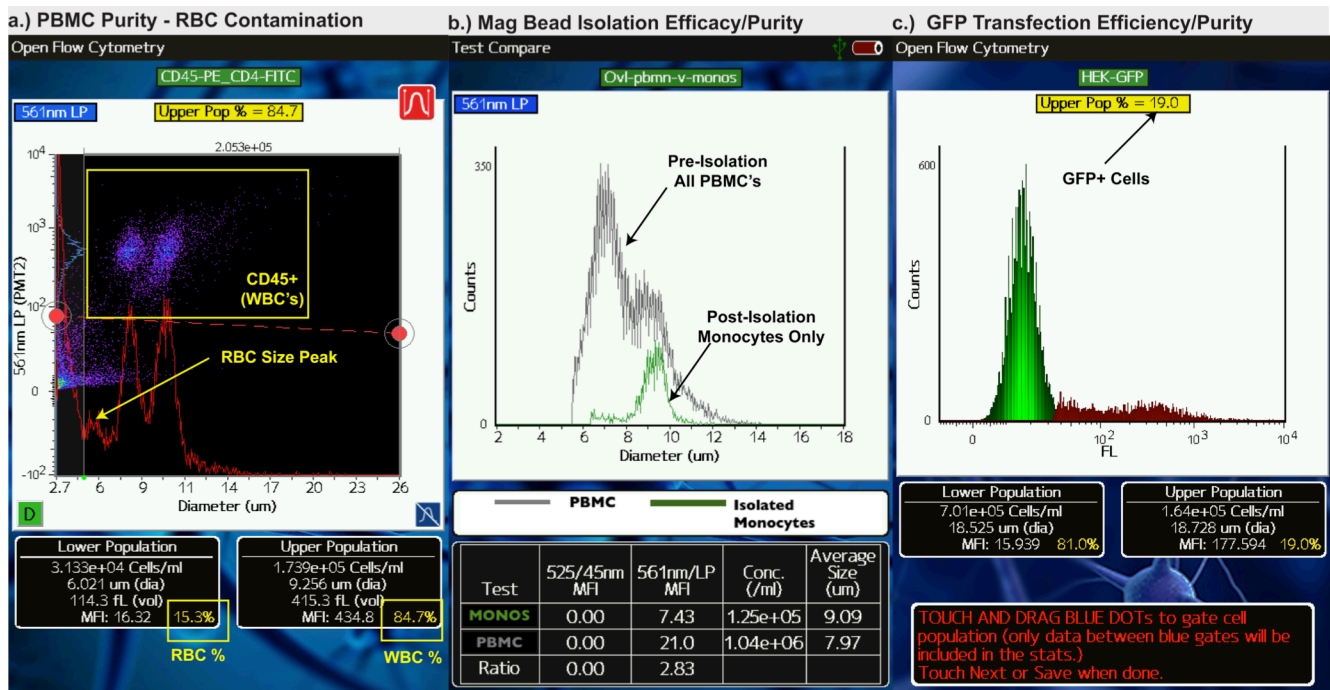


**Figure 6 – a.)** Moxi GO II Scatter plot output (PE fluorescence vs. cell size) of Ficoll-purified PBMC's, labeled with PE CD45 (HI30). The size histogram overlay (red curve) shows the size-differentiated RBC peak. The fluorescence separation (yellow box) highlights the fluorescently discriminated (CD45+) leukocytes. **b.)** Moxi Go II size histogram overlays comparing PBMC's immediately following Ficoll purification (gray curve) vs. the same cells following a magnetic bead purification of the monocyte population (green curve). In this case, the size-histogram alone is sufficient to verify the success of the magnetic bead isolation. **c.)** Representative fluorescence histogram output for GFP transfected (HEK) cells. The Moxi GO II system can provide a quick GFP+ cell check for verifying transfection and/or cell sorting efficiencies.

peripheral blood mononuclear cell (PBMC) preparation. For added clarity on the size resolution, a size histogram overlay (red trace) is enabled on the graph. As indicated by the yellow arrow, the RBC peak can be size-discerned in this sample allowing the user to readily calculate the degree of RBC “contamination” using the standard system size-gating approach. With the addition of fluorescence, the PBMC cells can also be labeled with a fluorophore for a second level of verification. **Figure 6a** shows an example of this secondary level of discrimination using a PE – CD45 (HI30) antibody label that fluorescently identifies all the leukocytes (manually indicated by yellow box around population).

A common technique for purification of cell samples for 10x cell preparations is to use magnetic bead columns with either enrichment or depletion strategies to purify cells by phenotype. **Figure 6b** shows this approach applied to isolating monocytes from a PBMC preparation. The figure shows a size-only histogram comparison of the initial PBMC prep (gray trace) compared to the post-isolation monocyte distribution (green trace). In this case, the sample purity can be readily verified with a simple, label-free measurement of the cell size distribution. Specifically, the smaller lymphocyte peak is no longer present, post-isolation. While added information can be obtained by combining the size measurement with a surface-label (e.g. PE CD14), in this case, the high-resolution of the Moxi GO II sizing allows the user to bypass the added preparation time associated with fluorescently labeling the cells.

The Moxi GO II system is also ideally configured (488nm excitation, 525/45nm PMT1 emission collection) for monitoring GFP-tagged protein transfection in cells. This is not only useful for determining the efficiency of GFP transfection but also, more relevant to 10x processing, can be used as a means of determining the purity of a sample sorted based on that transfected protein. **Figure 6c** provides an example fluorescent histogram output for HEK cells transfected with a GFP-tagged protein. In this case, the low level of transfected cells (19%, **Figure 6c** – Yellow Box) would provide the researcher with the strong warning to

redo the sort and/or transfection so that their time and material investments in 10x processing are not wasted.

### Precise/Accurate Nuclei Counts

For certain cell/sample types, achieving the necessary single cell suspension for proper single cell genomic analysis, can be challenging. In those cases, one recommended solution for 10x processing is to lyse the cells to achieve a suspension of isolated cell nuclei<sup>6,7,8</sup>. Isolating nuclei can avoid the detrimental effects of prolonged protease exposures and mechanical disruption procedures. Following isolation of the nuclei, it is still critical that the nuclei concentration be precisely measured and titrated so that, during the 10x droplet formation, each droplet contains only a single nucleus. For traditional cell counting approaches, counting nuclei is challenging due to their small size (typically 4-9µm diameter). Imaging system cell counters are incapable of reliably resolving such smaller sized particles (e.g. bead example in **Figure 5a**, bottom). Since the Moxi GO II's accurate sizing analysis accurately extends down to 3µm diameter particles, the system allows for quick, easy counting of isolated cell nuclei with the impedance detection approach alone. And, for an added dimension of nuclei resolution, the nuclei can also be quickly stained with PI to fluorescently separate the populations as well. An example of the nuclei counting capabilities of the Moxi GO II is shown in **Figure 7**. In this case, a Ficoll-purified PBMC sample was first run on the system. **Figure 7a** shows the scatter plot output of that test plotting the PI fluorescence (viability in this case) vs. the cell sizes. The PBMC's were subsequently exposed to a lysis protocol (Beckman Coulter, Zap-oglobin II reagent), isolating the nuclei. Running the lysed sample (**Figure 7b**) on the system yielded - the identical counts (1.23e5/ml) as with the intact cells. The size histogram overlay (**Figure 7**, red curves) show the shift in cell sizes. This quantitatively represented in the measured data below the scatter plot as well (303.9fL mean cell size for the intact PBMCs vs. 54.62fL for the isolated nuclei). The isolated nuclei also show the expected increase in fluorescence (population shifts up on the scatter plot) as the PI is no longer blocked from binding with the DNA by the intact (healthy) cell plasma membrane.

### Robust Cell Phenotyping

A final, broad area of cell characterization/QC of 10x cell preps is the use of cell surface immunolabeling techniques for phenotype analysis. This approach can be used to simply confirm or identify the cell composition prior to running genomic analysis (e.g. percent of CD8 positive T-Cells in a PBMC sample) or it can be used as another tool in determining the purity of the sample (e.g. using CD3 to determine the T-Cell purity following a T-cell sorting or magnetic -bead isolation procedure). With a seemingly limitless array of conjugated antibody clones, a vast array of cell phenotypes can be tracked. Traditional cell counting

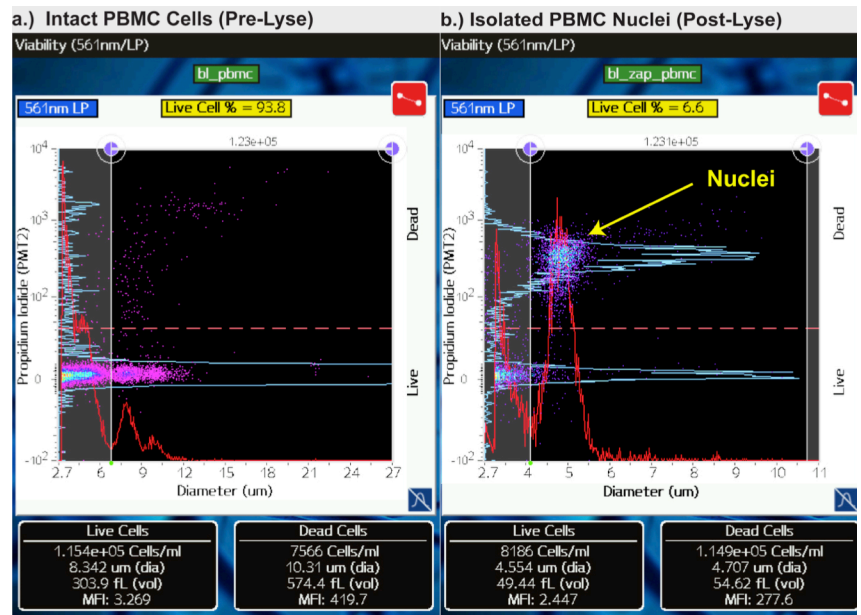


**Figure 7 – a.)** Ficoll-purified PBMCs, stained with PI and run on the Moxi GO II using the Cell Counts + Viability assay. **b.)** The same sample was lysed with Zap-oglobin II and the resulting nuclei prep was run on the Moxi GO II using the same assay. The system nuclei count was validated with an exactly equivalent count (as with the intact cells.) The size shift of the isolated nuclei (54.62fL) vs. the intact cells (303.9fL) provides further validation of the nuclei isolation

systems completely lack the capability for providing this valuable information. In contrast, the Moxi GO II has a 488nm laser and two PMT's, allowing for the simultaneous detection of two fluorophores (e.g. FITC and PE) to complement the precise Coulter-Principle counts and sizing. **Figure 8** shows two examples of phenotyping of Ficoll-purified PBMCs. Specifically, **Figure 8a** presents a dual label with FITC anti-human CD8 (HIT8a, BioLegend) and PE anti-human CD3 (OKT3, BioLegend). **Figure 8b** shows a separate example of PBMC's labeled with FITC-CD4 (SK3, BioLegend) and PE-CD4 (OKT3, BioLegend). In both cases, the fluorescence of the positive vs. negative populations is easily gated using the Moxi GO II quadrant gating tool, allowing the researcher to discriminate the cell populations fully on the two markers. For purity checks following sorting, the first PMT/channel (525/45nm) can be devoted to a unique antibody-label for the purified cells. The second channel, with the 646nm/LP filter, can be applied to measure PI-staining (viability). With that setup, the researcher immediately (with one test) achieves a broad array of QC: Phenotype purity, Size distribution (e.g. clustering), Concentrations, and Viability.

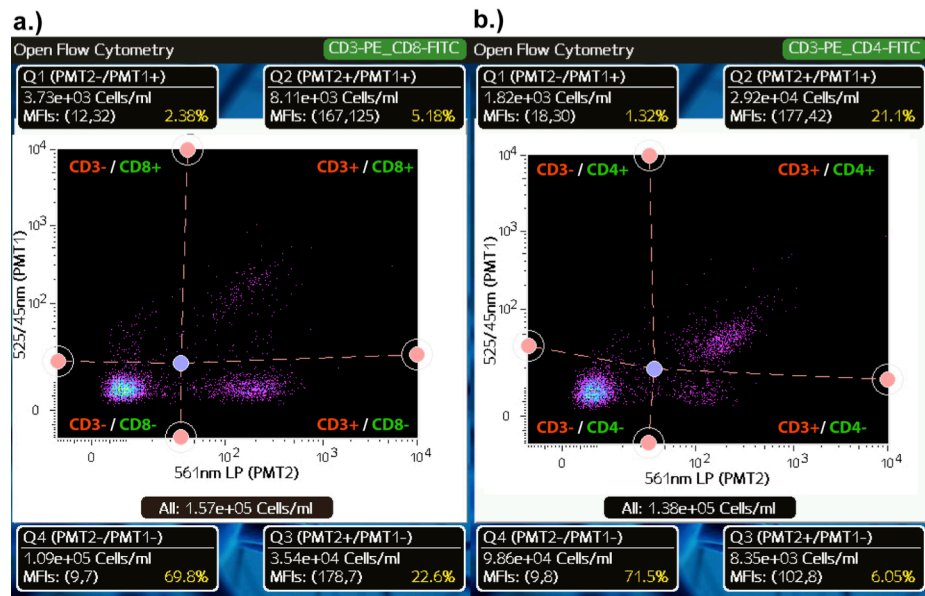


**Figure 8** – Moxi GO II measured FITC (PMT1, 525/45nm) vs. PE (PMT2, 561nm/LP) scatter plot output for Ficoll-Purified PBMC samples. a.) Dual-label with FITC anti-CD8 (HIT8a) and PE anti-CD3 (OKT3) antibody labels b.) Dual labeled with FITC anti-CD4 (SK3) and PE anti-CD3 (OKT3) antibody labels.

### Summary

Single cell genomic analysis has enabled far more precise and detailed insights into the genomic composition of cell and tissue samples. Towards that end, the 10x Genomics technologies have uniquely enabled the cell sample preparation that allows for genomic analysis on a single cell level. However, given the significant costs of both the 10x cell preparation step as well as the downstream sequencing, it is critical that researchers ensure proper sample composition prior to processing. To facilitate those preparations, 10x Genomics provides comprehensive guidance on the parameters necessary to achieve quality outputs with their 10x Chromium system.

Orflo's Moxi GO II system is uniquely suited towards monitoring, the broad array of QC metrics that will ensure successful 10 cell sample preparation. The diversity of parameters and the reliability of the data output of the Moxi GO II will help ensure that time, cost, and precious samples will not be wasted in downstream processing. Beyond the capabilities and quality of the data output discussed above, one of the most powerful features of the Moxi GO II instrument is the ease-of-use and versatility in collection of data. With an ability to run tests without the need for system warm-up, maintenance, or shutdown procedures, the Moxi GO II is ideally suited for instantaneous 10x cell sample QC checks. And, with a small system footprint, researchers can place the Moxi GO II in the culture hood or lab bench-top, granting a convenience that enables more immediate and frequent checks of their cell samples. These features should establish the Moxi GO II as a staple in any lab performing single cell genomic analysis using 10x Genomics technologies.



Work  
Smarter.

### References

1. Mikkelsen, T. Chromium Single Cell Solutions. in *ASHG Annual Meeting* (2016).
2. 10x Genomics. Single Cell Gene Expression - Chapter 4 - Sample Preparation. Available at: <https://www.10xgenomics.com/videos/>.
3. NYU Langone Genome Center. NYU Langone Health - Genome Technology Center Fees. Available at: <https://med.nyu.edu/research/scientific-cores-shared-resources/sites/default/files/genome-technology-center-pricing.pdf>.
4. Stanford Medicine. Stanford Medicine - Genome Sequencing Service Center - Rates. Available at: <http://med.stanford.edu/gssc/rates.html>.
5. University of Michigan. University of Michigan - DNA Sequencing Core Price List.
6. Hwang, B., Lee, J. H. & Bang, D. Single-cell RNA sequencing technologies and bioinformatics pipelines. *Exp. Mol. Med.* **50**, 96 (2018).
7. Nguyen, Q. H., Pervolarakis, N., Nee, K. & Kessenbrock, K. Experimental Considerations for Single-Cell RNA Sequencing Approaches. *Front. cell Dev. Biol.* **6**, 108 (2018).
8. 10x Genomics. SAMPLE PREPARATION TIPS FOR SINGLE CELL GENE EXPRESSION.



Work  
Smarter.